Study of the Electrochemical Reduction of Dioxygen in Acetonitrile in the Presence of Weak Acids

Pradyumna S. Singh and Dennis H. Evans*

Department of Chemistry, University of Arizona, Tucson, Arizona 85721

Received: September 18, 2005; In Final Form: November 6, 2005

The electrochemical reduction of dioxygen has been studied in acetonitrile at glassy-carbon electrodes. The initial step is the reversible one-electron reduction to form superoxide. In the presence of hydrogen-bond donors (water, methanol, 2-propanol), the superoxide forms a complex with the donor resulting in a positive shift in the potential that can be analyzed to obtain formation constants for these complexes. Stronger acids result in protonation of the superoxide followed by reduction to produce HO_2^-. In the absence of hydrogen-bond donors, the reduction of superoxide occurs at very negative potentials, and this second reduction peak is very much drawn-out along the potential axis, indicating a small value of the transfer coefficient, α. The addition of hydrogen-bond donors, HA, brings about a positive shift in this peak, without a noticeable change in shape. The reaction occurring at the second peak is a concerted proton and electron transfer (CPET) in which the electron is transferred to superoxide and a proton is transferred from HA to the superoxide, forming HO_2^- and A^- in a concerted process. An estimation of the standard potential for this reaction shows that the second reduction always occurs at a high driving force, which explains the small value of α that is observed. Consistent with a CPET, a kinetic isotope effect, HA versus DA, was detected for the three hydrogen-bond donors. The increasing positive shift of the second peak with increasing water concentration has been interpreted as being a consequence of the change in the formal potential, as water is both a reactant in the process and a participant through the hydrogen-bond stabilization of the anions.

1. Introduction

The various electrode reactions of dioxygen, involving both its reduction and its generation, have been extensively studied for decades.[1] The interest in these reactions stems from their importance in areas such as fuel cells and corrosion. The biological processes of respiration and photosynthesis, while not directly involving electrochemistry, do depend on the energetics and kinetics of the reactions that are a part of the redox processes of dioxygen.[2,3]

In this paper we will focus upon the reduction of dioxygen. The electrochemical reduction in aqueous media is rather well understood.[1] There are two principal overall reactions: the two-electron reduction to hydrogen peroxide and the four-electron reduction to water. The former is generally favored in alkaline media and with noncatalytic electrodes such as mercury and gold.[1] The one-electron reduction to form the anion radical (superoxide) is not seen on metal electrodes in aqueous media, regardless of the pH. This is somewhat surprising because one might expect superoxide to be stable in alkaline media where it would not undergo protonation and further reaction since the pK_a of hydroperoxyl ($HO_2^\bullet$) is 4.8 in water.[4] Nevertheless, the disproportionation of superoxide is quite rapid in water (reactions 1 and 2), which could account for the overall two-electron reduction to hydrogen peroxide that is normally seen.

$$O_2 + e^- \rightleftharpoons O_2^{-\bullet} \quad (1)$$

$$2O_2^{-\bullet} + H_2O \rightleftharpoons O_2 + HO_2^- + OH^- \quad (2)$$

However, the homogeneous disproportionation reaction is not fast enough to explain the exclusive two-electron character of the reduction in aqueous media.[5]

Nevertheless, the formation of superoxide in aqueous media is readily observed when modified electrodes are used. In early work,[5−8] organic adsorbates were added to the solution, and the one-electron reduction of dioxygen to superoxide was detected. Later, Yang and McCreery[9] reported the detection of superoxide in alkaline media upon reduction of dioxygen at a glassy-carbon electrode that had been modified by the attachment of a layer of 4-methylphenyl radicals. Also, Matsumoto et al.[10] observed the formation of superoxide upon reduction of dioxygen at alkanethiol-modified gold electrodes in alkaline aqueous solutions. Thus, a modified electrode surface allows the true kinetics of the disproportionation of superoxide to be examined. Its very fast disproportionation at unmodified metal surfaces can be attributed to a double-layer effect or interactions of superoxide with the metal surface.

In contrast, the reduction of dioxygen to superoxide is readily observed in nonaqueous media,[11−17] including room-temperature ionic liquids.[18−21] Superoxide is relatively stable in solvents such as acetonitrile (ACN), *N*,*N*-dimethylformamide (DMF), and dimethyl sulfoxide (DMSO), and reaction 1 proceeds with chemical reversibility on various metal surfaces. The electron-transfer reversibility, however, ranges from high on mercury and glassy carbon to low on most other metal electrodes.

* To whom correspondence should be addressed. E-mail: dhevans@email.arizona.edu.

10.1021/jp055296f CCC: $33.50
Published on Web 12/15/2005

The effect of added proton donors, HA, on the dioxygen/superoxide process has been studied,[15,22,23] and, for sufficiently acidic additives, the following reaction sequence is indicated:

$$O_2 + e^- \rightleftharpoons O_2^{-\bullet} \quad (1)$$

$$O_2^{-\bullet} + HA \rightleftharpoons HO_2^{\bullet} + A^- \quad (3)$$

$$HO_2^{\bullet} + O_2^{-\bullet} \rightleftharpoons HO_2^- + O_2 \quad (4)$$

Thus, the addition of HA will convert the one-electron reduction of dioxygen to an overall two-electron process producing hydroperoxide anion.

Very little attention has been directed to the reduction of superoxide in nonaqueous media in the absence of added proton donors. Goolsby and Sawyer[24] noted that superoxide was reduced at −2 V versus SCE in DMSO, while Vasudevan and Wendt[25] saw a similar reduction process in DMSO as well as DMF and ACN. These authors assumed that the process is the reduction of superoxide to O_2^{2-} followed by rapid protonation to give HO_2^-, the latter reaction causing the overall reaction to be irreversible. Recently Guo and Lin[26] studied the reduction of dioxygen in anhydrous ACN using ultrafast cyclic voltammetry and were able to detect an apparently reversible reduction feature near −2.8 V versus ferrocene/ferrocenium that might be due to the $O_2^{-\bullet}/O_2^{2-}$ couple.

In this paper we present the results of studies of both steps of the reduction of dioxygen in ACN as solvent. The results were obtained in both the absence and the presence of the weak proton donors (water, 2-propanol, methanol and 2,2,2-trifluoroethanol (TFE)) as well as the stronger acid 4-*tert*-butylphenol. In this work we demonstrate that the reduction of superoxide in the presence of the weak proton donors (HA) occurs by a concerted proton and electron-transfer reaction (CPET)[27] with a hydrogen bonded complex composed of superoxide and HA as the reactant. A preliminary report with results in DMF has appeared.[27b]

2. Experimental Section

2.1. Chemicals and Reagents. Anhydrous ACN (Aldrich, 99.8%; 0.001% H_2O) was used as received. It was transferred into the cell via cannula under nitrogen. Tetrabutylammonium hexafluorophosphate (Bu_4NPF_6), was recrystallized three times from ethanol. Tetramethylammonium hexafluorophosphate (Me_4NPF_6; Aldrich) was recrystallized from ACN−water mixtures (9:1), and sodium perchlorate ($NaClO_4$; Aldrich) was used as received. The electrolytes were dried overnight at 90 °C in a vacuum oven before each experiment. In all experiments, the concentration of the supporting electrolyte (Bu_4NPF_6 and $NaClO_4$) was 0.10 M. The concentration of Me_4NPF_6 was 0.050 M because of its low solubility in ACN. The Bu_4NPF_6 employed in the kinetic isotope experiments was obtained from Fluka (puriss electrochemical grade, 99.0%) and was used as received. The background near cathodic breakdown was somewhat lower with this electrolyte than it was with the recrystallized material.

Water was prepared in a Millipore Milli-Q apparatus. Anhydrous methanol (CH_3OH; 99.8%, Aldrich), anhydrous 2-propanol ($(CH_3)_2CHOH$; 99.5%, Aldrich), TFE (99.5%, Aldrich), 4-*tert*-butylphenol (99%; Aldrich), aqueous hydrogen peroxide (H_2O_2; 30%, EMD), and tetrabutylammonium hydroxide (1.0 M in methanol; Aldrich) were used as received. Deuterated water (D_2O; 99.9%D, Cambridge Isotopes), deuterated methanol (CH_3OD; 99.5%D, Aldrich), and deuterated 2-propanol ($(CH_3)_2CHOD$; 98%D, Aldrich) were also used as received. For the cases in which H_2O, CH_3OH, $(CH_3)_2CHOH$, TFE, and 4-*tert*-butylphenol were added incrementally to the electrochemical cell, a 10 mL stock solution was prepared by dissolving the additive in a solution of 0.10 M Bu_4NPF_6/ACN. Required quantities were then pipetted into the cell, depending upon the desired molar concentrations of the additives to be achieved.

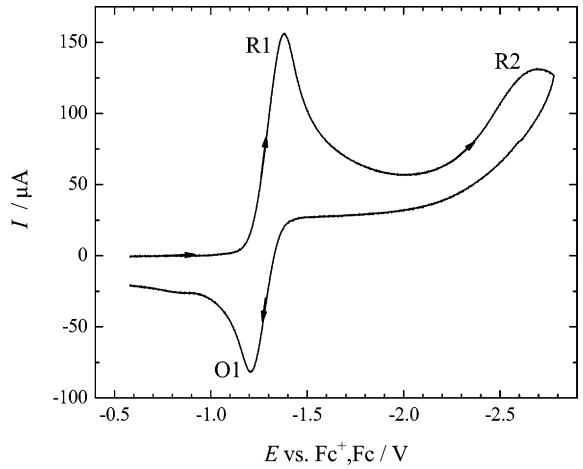

Figure 1. Voltammogram of dry, air-saturated ACN with 0.10 M Bu_4NPF_6 at a glassy-carbon electrode. Scan rate: 0.50 V/s. Temperature: 298 K.

2.2. Electrochemical Cells, Electrodes, and Instrumentation. The electrochemical cell was water-jacketed, and the temperature was maintained at 25 °C. The volume of the cell used was 20 mL. The working electrode was normally a 3-mm diameter glassy-carbon electrode (Bioanalytical Systems). In some experiments a 2-mm diameter platinum electrode or a 3-mm diameter gold electrode was used. The counter electrode was a coil of platinum wire (99.99%). The home-built reference electrode was a silver wire in contact with a solution of 0.10 M Bu_4NPF_6 and 0.010 M $AgNO_3$, in ACN. The reference electrode was separated from the contents of the cell by means of a porous Vycor frit. When not in use, the reference electrode was kept immersed in the above solution at all times to prevent the drying of the frit.

The working, reference, and counter electrodes were held in the same relative position to each other throughout all the experiments performed to ensure that the uncompensated solution resistance remained constant. The counter electrode was especially positioned sufficiently far away from the working electrode to enable a uniform current density at the working electrode. Prior to all experiments the working electrode was polished on a polishing wheel with 5.0-μm alumina paste (aqueous, Buehler) followed by 0.3- and 0.05-μm aqueous alumina. The electrode was rinsed with deionized water and sonicated for fifteen minutes, rinsed again, and finally rinsed with acetone. After air-drying, the electrode was ready to use. Preconditioning the electrode led to reproducible results. Specifically, before each set of experiments, the electrode potential was scanned about 10 times over the entire potential range used in Figure 1. In the presence of hydrogen-bond donors, three scans were found to be sufficient.

The reference electrode was frequently calibrated with reference to the ferrocenium ion/ferrocene couple (Fc^+/Fc). This was accomplished by obtaining voltammograms of ferrocene using the reference electrode and determining the potential of the ferrocene couple with respect to the reference by simulation of the voltammograms. In accordance with the recommendation

of the IUPAC,[28] all potentials reported here are referenced to the potential of this couple.

The source of oxygen was air (21% oxygen). The solubility of pure oxygen (1 atm) in ACN was determined[29] to be 8.1 mM at 298 K. Thus the concentration of dioxygen in our air-saturated solutions was 1.7 mM. To measure the background current, which includes nonfaradaic currents due to the charging of the double-layer and other sources, the electrolyte solution was purged with dinitrogen (Air Liquide, 99.995%) for 20 min prior to any measurements. The dinitrogen was saturated with solvent by bubbling through anhydrous ACN and was passed through anhydrous calcium sulfate before being introduced into the cell. All experiments were performed with a model 273 EG&G Princeton Applied Research potentiostat.

The uncompensated solution resistance, R_u, for 0.10 M Bu_4NPF_6 was determined from fits of simulations to voltammograms of ferrocene. The voltammograms were obtained for a series of scan rates, and simulation was performed by keeping the electron-transfer rate constant, k_s, sufficiently high such that any change in peak separation, ΔE_p, could be attributed entirely to the resistance, R_u. It was determined that the resistance for the GC electrode in our cell arrangement was 180 Ω. In studies of dioxygen, this solution resistance was partially compensated (140 Ω) using positive feedback. The remaining solution resistance (40 Ω) was included as a simulation parameter when analyzing data. A similar measurement of solution resistance was made for a solution of ACN containing 500 mM H_2O, giving 190 Ω.

When acquiring data at scan rates less than 0.10 V/s, the 5.3 Hz filter on the PAR 273 was used. Between 0.1 and 5 V/s, the 590 Hz filter was used, and above 5 V/s no filtering was applied. Digital simulations were performed on the background-corrected data using DigiSim (version 3.03) from Bioanalytical Systems. Operating conditions for the simulation program were spherical diffusion (to mimic edge diffusion to the disk[30]), 0.002 V stepsize and 0.50 for the expanding grid factor. Electron-transfer reactions were treated by either Butler−Volmer kinetics, with the standard rate constant and transfer coefficient as kinetic parameters, or by the so-called Marcusian treatment, with the standard rate constant and reorganization energy as kinetic parameters. The type of treatment used will be mentioned at each instance of the application of DigiSim.

3. Results and Discussion

3.1. First Step of Reduction. Figure 1 displays a voltammogram of air-saturated ACN at a glassy-carbon electrode. On the initial negative-going scan, the reduction of dioxygen to superoxide occurs at peak R1, which is followed by a second, very drawn-out, irreversible reduction peak, R2. On the return sweep, the oxidation of superoxide to dioxygen occurs at peak O1. An almost imperceptible anodic peak near −0.8 V is seen only after excursions through R2. If the scan is reversed just past R1, only the quasireversible R1/O1 pair of peaks appears in the voltammogram.

Voltammograms showing only peaks R1 and O1 are presented in Figure 2 for no added water and for the addition of 82 and 165 mM water. Changes in the shape and height of the peaks in Figure 2 are minor. The only important change is the positive shift in potential as the concentration of water is increased. As mentioned in the Introduction, we will show that the reduction of superoxide in the presence of water and other weak acids is a CPET with a hydrogen-bonded acid−superoxide complex as the reactant. By studying the effect of water on the first step of reduction, we were able to determine formation constants for these complexes.

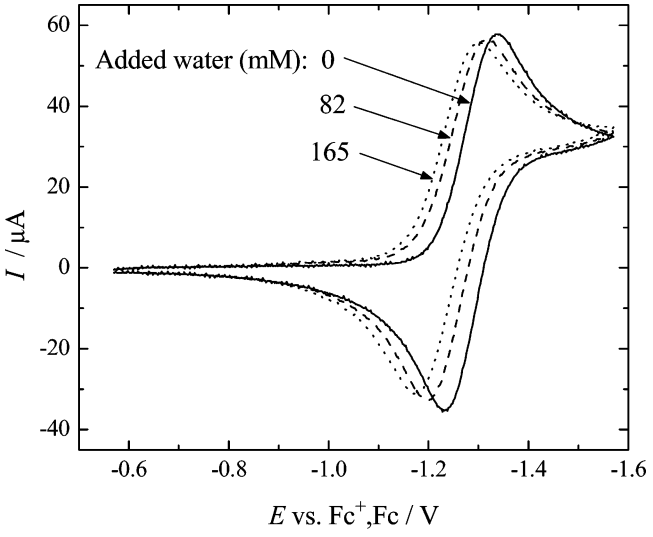

Figure 2. Voltammograms with added water. Scan rate: 0.050 V/s. Other conditions are the same as those shown in Figure 1.

The electrode reaction is the one-electron reduction to form superoxide, reaction 1:

$$O_2 + e^- \rightleftharpoons O_2^{-\bullet} \quad (1)$$

This is followed by the formation of 1:1 and 1:2 complexes with formation constants K_1 and K_2:

$$O_2^{-\bullet} + HA \rightleftharpoons (O_2^{-\bullet})\cdot(HA) \;\; K_1 \quad (5)$$

$$(O_2^{-\bullet})\cdot(HA) + HA \rightleftharpoons (O_2^{-\bullet})\cdot(HA)_2 \; K_2 \quad (6)$$

The observed formal potential in the presence of HA, $E^\circ_{1,HA}$, is related to the standard potential with no HA, E°_1, the concentration of HA, C_{HA}, and the formation constants given by eq 7,[31] which assumes no binding of dioxygen by HA.

$$E^\circ_{1,HA} = E^\circ_1 + \frac{RT}{F}\ln[1 + K_1C_{HA} + K_1K_2C_{HA}^2] \quad (7)$$

Values of $E^\circ_{1,HA}$ were determined as the average of the peak potentials for R1 and O1, and the results were plotted versus the logarithm of the water concentration (Figure 3).

Also included in Figure 3 is the fit of eq 7 to the data for water with $E^\circ_1 = -1.286$ V, $K_1 = 20$ M^{-1}, and $K_2 = 5$ M^{-1}. Fits with $K_2 = 0$ were inferior, but one cannot be certain that the small value found, 5 M^{-1}, is meaningful.

It might be expected that these formation constants would be larger for weak acids that are more acidic. Little is known about the pK_a values in ACN, but for DMSO pK_a = 31.2 for water, 30.25 for 2-propanol, and 29.0 for methanol.[32] When 2-propanol was used as an additive, again there was little change in the peak shape, and a positive shift in the formal potential was observed as the concentration was increased. A plot of $E^\circ_{1,HA}$ versus the logarithm of the 2-propanol concentration is also given in Figure 3, along with the fit to the data according to eq 7 with $E^\circ_1 = -1.286$ V, $K_1 = 15$ M^{-1}, and $K_2 = 0$ M^{-1}; that is, the inclusion of the 1:2 complex did not improve the fit. Similarly, the results for methanol (Figure 3) were fit by $E^\circ_1 = -1.286$ V, $K_1 = 30$ M^{-1}, and $K_2 = 3$ M^{-1}.

Data for the formation constants are tabulated in Table 1. Also included are results for the deuterated analogues of the three acids. The fact that these formation constants are indistinguishable from those for their protiated counterparts

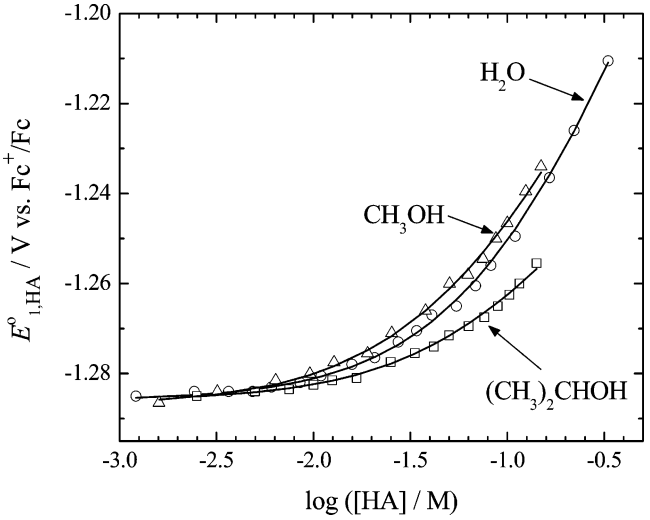

Figure 3. Formal potentials for the first step of reduction as functions of the concentration of added weak acids, HA. Points: experimental. Curves: Fits of eq 7 to the data using formation constants given in Table 1.

TABLE 1: Formation Constants of Superoxide with Weak Acids[a]

acid	K_1/M^{-1}	K_2/M^{-1}
water	20 (19)	5 (5)
2-propanol	15 (14)	
methanol	30 (27)	3 (4)

[a] Numbers in parentheses are for deuterated acid. Uncertainties in K_1 estimated to be ±10%. No estimate available for K_2. Inclusion of the values shown for water and methanol resulted in a net improvement of the fits.

indicates that there is no equilibrium isotope effect in these complexation reactions.

The values of the formation constants can be used to construct species distribution plots. Figure 4 shows such a plot for water. Here one can see the fractions of the total superoxide concentration that are present as $O_2^{-\bullet}$, $(O_2^{-\bullet})(H_2O)$, and $(O_2^{-\bullet})(H_2O)_2$. Substantial fractions of superoxide are present as 1:1 and 1:2 complexes at water concentrations greater than about 0.05 M, so one or both are candidates for the reactant at the second peak. Even though they do not represent 100% of the superoxide concentration, they are kinetically reasonable reactants because the formation and dissociation of hydrogen-bonded complexes is expected to be very rapid.

TFE is a much stronger acid than the three acids considered so far ($pK_a = 23.45$ in DMSO[32]). Accordingly, it showed a much larger value of K_1 (200−300 M^{-1} from the shifts in the R1/O1 for up to 15 mM added TFE). As will be seen in detail later, high concentrations of all of the additives have the effect of shifting peak R2 in the positive direction. TFE is much more effective in moving the peak, even at concentrations as low as 4 mM (Figure 5). It turns out that the approximately 12% increase in the peak height observed for R1 upon going from 0 to 15 mM added TFE is due entirely to the encroachment of the second peak on the first, as shown by simulation. It is not due to the interference of the prior protonation process (reaction 3) followed by electron transfer (reaction 4). This is interesting because the pK_a of hydroperoxyl ($HO_2^{\bullet}$) is 22.8 in DMF,[27] which suggests that superoxide might be a strong enough base to obtain a proton from TFE.

The peak near −2.7 V that is seen with the highest concentration of TFE, and which seems to have replaced R2,

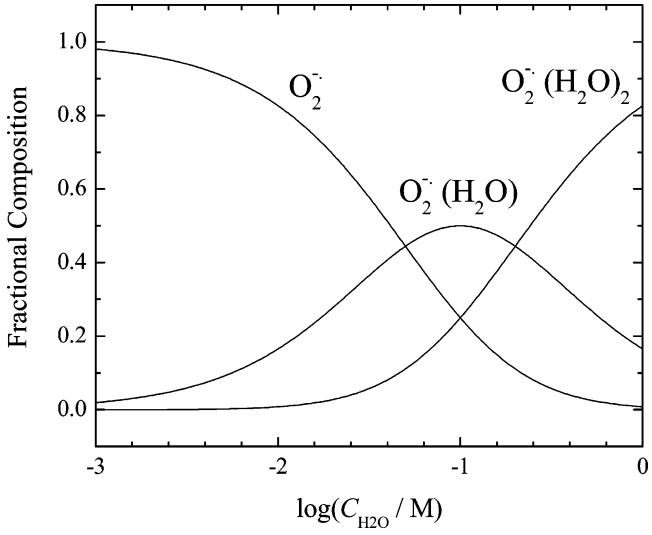

Figure 4. Species distribution diagram for the superoxide−water system calculated using the formation constants from Table 1.

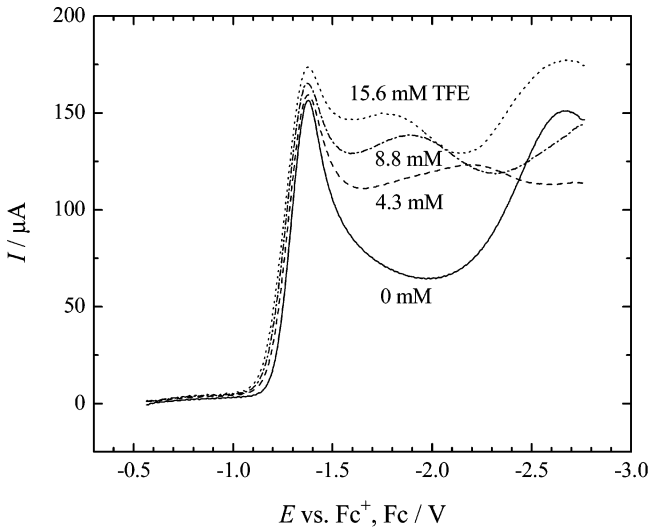

Figure 5. Voltammograms of air-saturated ACN with added TFE. Other conditions are the same as those shown in Figure 1.

is actually due to the reduction of hydrogen peroxide formed during the prior two peaks. The beginning of this peak is seen at 8.8 mM.

The addition of the stronger acid, 4-*tert*-butylphenol (data not shown), brought about changes that were in agreement with earlier studies in DMSO.[22] Its pK_a is 19 in DMSO.[33] That is, 4-*tert*-butylphenol is a strong enough acid to cause the mechanism to change to reactions 3 and 4, proton transfer preceding electron transfer.

3.2. Second Step of Reduction. As can be seen in Figure 1, the second step of the reduction of dioxygen (R2) is very drawn-out along the potential axis. Upon the addition of increasing amounts of water (or methanol, 2-propanol or TFE; Figure 5), R2 moves in the positive direction. This is shown for water in Figure 6 (similar data for methanol and 2-propanol not shown). It is noteworthy that the shift in the potential of R2 is not accompanied by any significant change in peak shape. That is, the transfer coefficient is independent of the water concentration. The shifts seen for the three weak acids at 0.5 M concentration are 0.8 V for water, 0.5 V for 2-propanol, and 1.0 V for methanol.

We propose, in accordance with the interpretation made earlier,[27] that the reaction responsible for R2 is the CPET to

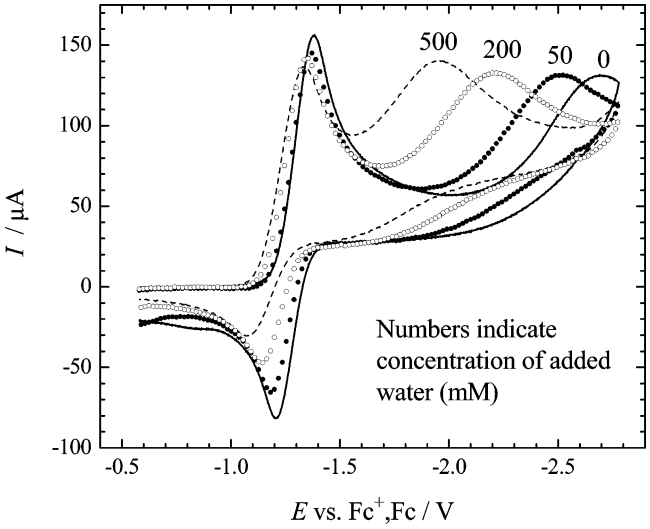

Figure 6. Voltammograms of air-saturated ACN with added water. Other conditions are the same as those shown in Figure 1.

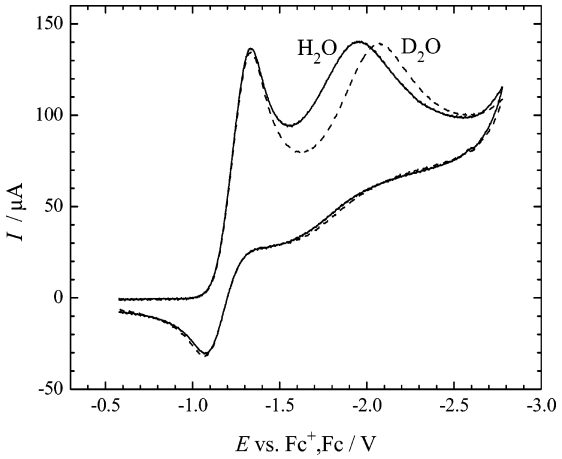

Figure 7. Voltammograms of air-saturated ACN in the presence of 0.50 M H_2O or D_2O. Other conditions are the same as those shown in Figure 1.

the hydrogen-bonded complex of superoxide with water (or other weak acid), reaction 8. A significant H/D kinetic isotope effect (KIE) was observed in DMF with water as the additive,[27] and this was also found to be true in ACN for water, 2-propanol, and methanol. Results for water are shown in Figure 7 for 0.50 M added H_2O (solid) and D_2O (dashed). As noted earlier, the first peak is virtually identical for the two isotopes. The peak potential of R2 is a function of the standard potential, transfer coefficient, and standard rate constant for reaction 8, where the presumed reactant is the 1:1 complex (illustrated for H_2O).

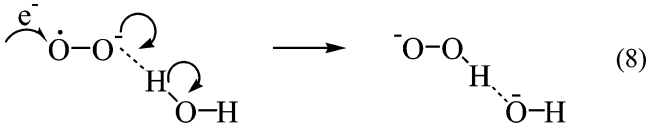

(8)

The standard potential should be the same for H_2O and D_2O as additives (no thermodynamic isotope effect), and the apparent value of α is virtually the same as that judged by the nearly identical shape of peaks R2 in Figure 7. Therefore, we attribute the difference in peak potential to differences in the standard rate constant, k_s. The more negative peak potential for D_2O compared to H_2O means that the rate constant is smaller for the former, which is the proper trend for a KIE. The difference in peak potentials, $E_{p,H} - E_{p,D}$, can be combined with the

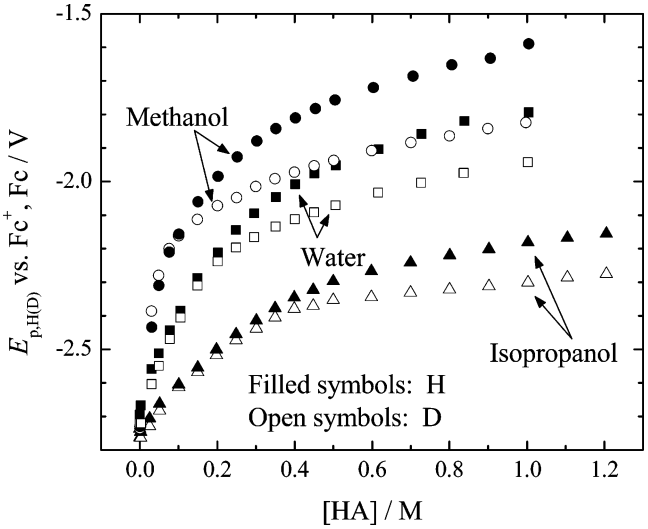

Figure 8. Peak potential of peak R2 as a function of the concentration of protiated (solid symbols) and deuterated (open symbols) additives. Other conditions are the same as those shown in Figure 1.

TABLE 2: KIEs for the Reduction of Superoxide−Weak Acid Complexes[a]

concentration of CH_3OH (CH_3OD) (M)	$k_{s,H}/k_{s,D}$	concentration of H_2O (D_2O) (M)	$k_{s,H}/k_{s,D}$	concentration of $(CH_3)_2CHOH$ ($(CH_3)_2CHOD$) (M)	$k_{s,H}/k_{s,D}$
0.20	1.9				
0.25	2.4				
0.30	2.7	0.30	1.7		
0.35	3.0	0.35	1.9		
0.40	3.2	0.40	2.2	0.40	1.3
0.45	3.5	0.45	2.4	0.45	1.4
0.50	3.7	0.50	2.4	0.50	1.5
0.60	4.0	0.62	2.6	0.60	1.8
0.70	4.3	0.73	2.9	0.70	2.0
0.80	4.7	0.84	3.1	0.80	2.1
0.90	4.6			0.90	2.3
1.00	5.6	1.00	3.0	1.00	2.4
				1.10	2.4
				1.20	2.4

[a] Calculated using eq 9 from the data in Figure 8 and $\alpha = 0.19$.

common value of α (0.19) to obtain the ratio of the rate constants according to eq 9 in which the subscripts H and D refer to H_2O and D_2O, respectively. Equation 9 is based on the Butler−Volmer formulation of electron-transfer kinetics.[34a] The KIE is defined as $k_{s,H}/k_{s,D}$ and was found to be 2.4 for 0.50 M. This may be compared to the value of 2.5 found for DMF.[27b]

$$\frac{k_{s,H}}{k_{s,D}} = \exp\left[\frac{\alpha F}{RT}(E_{p,H} - E_{p,D})\right] \qquad (9)$$

Peak potentials for various concentrations of H_2O/D_2O are presented in Figure 8 along with data for CH_3OH/CH_3OD and $(CH_3)_2CHOH/(CH_3)_2CHOD$. No KIE is seen at low concentrations of the additives, but it becomes prominent above ~0.2 M for methanol, 0.3 M for water and 0.4 M for 2-propanol. The KIE for all three additives as obtained through eq 9 are summarized in Table 2. A significant increase in KIE with increasing concentration is seen for all three additives, and the concentration where the effect first appears parallels the formation constants for the 1:1 complex (Table 1). That is, the KIE develops at concentrations of additives where the concentrations of complexes are becoming significant.

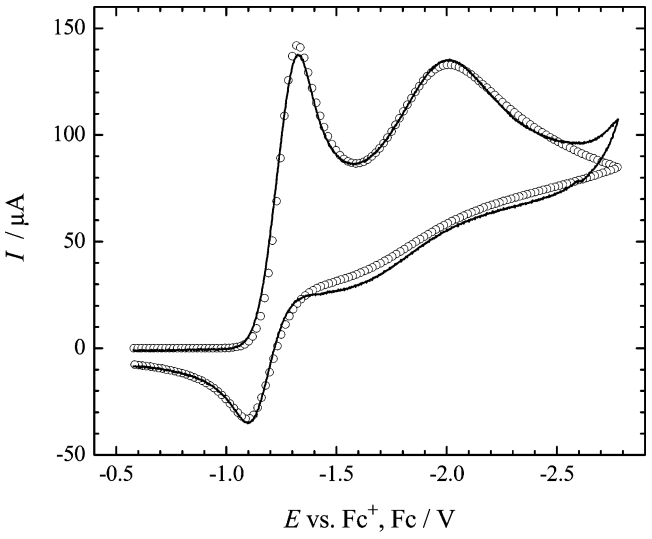

Figure 9. Comparison of simulation (points) with background-corrected voltammogram (line) for air-saturated ACN with 0.40 M added water at 0.50 V/s. Simulation parameters: $E_2^{\circ\prime} = -0.56$ V; $k_s = 5 \times 10^{-10}$ cm/s; $\lambda = 1.8$ eV.

The entire voltammogram can be fit by digital simulation in which the R1/O1 process is treated as a quasireversible reaction with the standard potential and formation constants for the fast complexation reactions determined earlier. The second step of reduction, producing R2, was treated as totally irreversible in one of two ways: either by Butler−Volmer kinetics in which the electron-transfer rate constant and transfer coefficient are variables or by a treatment due to Marcus in which the transfer coefficient is a function of potential according to eq 10 where λ is the reorganization energy.[34b] The form of this relationship is also correct for CPET.[27c]

$$\alpha = \frac{1}{2} + \frac{F(E - E^\circ)}{2\lambda} \tag{10}$$

Both of these approaches work well, and an example of the latter is given in Figure 9. The fact that a constant value of α can be used to describe peak R2 by the first method arises from the fact that the main part of the peak does not encompass a large enough potential region for α to change appreciably. It is noteworthy that the height of peak O1 is well matched, indicating that the mechanism correctly accounts for the formation and loss of the superoxide species. The rising current past −2.5 V is due to the reduction of the hydrogen peroxide formed during passage through the preceding two peaks. This reaction was not included in the simulation.

The small value of α that was found (0.19) is indicative that peak R2 is situated far negative of the standard potential of reaction 11, which was calculated to be −1.03 V versus Fc^+/Fc (see Supporting Information for details). For example, with 1.0 M water added, the peak potential of R2 is −1.8 V. Thus, peak R2 does occur at high driving force, and the magnitude of α is reasonable.

$$O_2^{-\bullet} + H_2O + e^- \rightleftharpoons HO_2^- + OH^- \tag{11}$$

According to eq 10, at any given water concentration, the value of α will become smaller as the potential of R2 is caused to be more negative. This was achieved for 500 mM added water by increasing the scan rate from 0.02 V/s to 100 V/s. When the voltammograms were fit by simulations using Butler−Volmer kinetics, the apparent α values decreased as the scan rate increased (and the peak potential became more negative). Selected results are (scan rate (V/s), peak potential (V), α) 0.02, −1.822, 0.23; 0.1, −1.841, 0.21; 1, −1.963, 0.19; 10, −2.125, 0.17; and 100, −2.387, 0.16. Thus, the expected decrease in α with increased driving force is fully borne out by experiment.

The process occurring at R2 has been described as a CPET. How can we exclude the stepwise process of electron transfer followed by a separate fast protonation reaction? The effect of such a reaction following electron transfer is to shift the peak in the positive direction from the standard potential for the preceding electron transfer. According to eq 10, the value of α would then be larger than one-half, precisely the opposite of what is seen.

We must now inquire into the reasons for the monotonic positive shift in the peak potential for R2 (Figure 8) that is seen for all three additives. This question was addressed by simulations using λ, k_s, and E° as variables with a potential-dependent transfer coefficient according to eq 10. It was reasoned that both λ and k_s should depend only on the nature of the reactant and solvent and not on the concentration of the hydroxylic additive. Thus, the shift in potential must be associated with a change in the formal potential as the concentration of water is increased. One aspect of this change is transparent: because water is a reactant, the formal potential must shift 59 mV in the positive direction for every 10-fold increase in the water concentration (assuming that the 1:1 complex is the reactant).

However, there are other factors. To calculate the formal potential, one must use the actual concentrations, viz., 1.7 mM superoxide reacts to form 1.7 mM HO_2^- and 1.7 mM $OH^{-\bullet}$ Other factors are the complexation of superoxide, HO_2^-, and OH^- by the added water. We will base our analysis on the formation of the specific complexes of these species with water though treatment in terms of increased solvation energies with the addition of water that could also be performed. The Nernst equation for reaction 11 is eq 12 in which activities have been replaced by molar concentrations. Here, E_2° is the standard potential of the second step of reduction.

$$E = E_2^\circ + \frac{RT}{F}\ln\left(\frac{[O_2^{-\bullet}][H_2O]}{[HO_2^-][OH^-]}\right) \tag{12}$$

The fraction of the species j present as the free, uncomplexed form is indicated by f_j. Let C be the common concentration of superoxide, HO_2^-, and OH^- being considered (1.7 mM) and, for example, represent $[O_2^{-\bullet}]$ by $f_{O_2^-}C$. When the concentrations according to the conditions of the reaction are placed in eq 11, the potential, E, will be the formal potential, $E_2^{\circ\prime}$. For this analysis, we considered only the 1:1 complex so that $f_{O_2^-}$ was

$$E_2^{\circ\prime} = E_2^\circ + \frac{RT}{F}\left[\ln[H_2O] - \ln C + \ln\frac{f_{O_2^{-\bullet}}}{f_{HO_2^-} f_{OH^-}}\right] \tag{13}$$

given by $1/(1 + K_1[H_2O])$.

To implement this analysis, simulations were performed with constant λ and k_s for all of the added water concentrations. The value of the standard potential was allowed to vary in order to optimize the fits. To establish the values of λ and k_s to use, simulations with small concentrations of water were studied using the formal potential (eq 13) with the f-values set at unity because there should be little hydrogen-bond association at low concentrations. Once these values of λ and k_s were established, namely, $\lambda = 1.8$ eV and $k_s = 5 \times 10^{-10}$ cm/s, they were held constant and only $E_2^{\circ\prime}$ was allowed to vary in fitting the simulations to the data. The resulting plot of $E_2^{\circ\prime}$ versus the

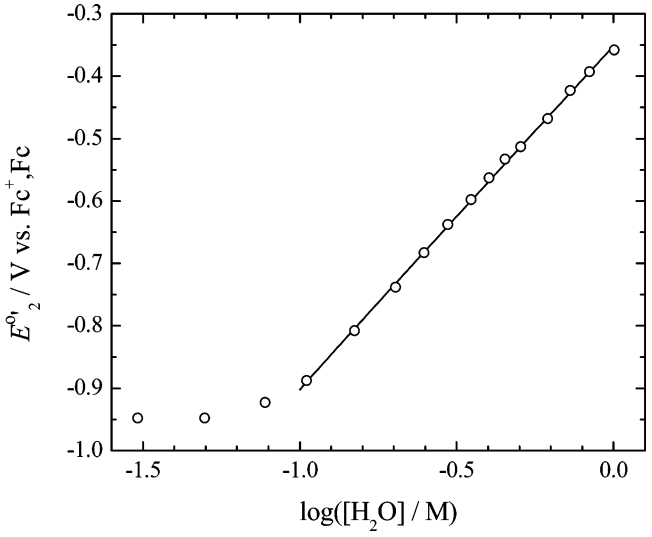

Figure 10. Formal potential for the second step of reduction, $E_2^{\circ\prime}$ as evaluated from simulations such as that in Figure 9 as a function of water concentration (symbols). Line: $E_2^{\circ\prime}$ calculated from eq 13 using $f_{HO_2^-}f_{OH^-}$ found in the simulations for 0.1−1.0 M added water.

logarithm of the concentration of water is shown in Figure 10. A smooth positive shift in $E_2^{\circ\prime}$ begins around 0.1 M water and the plot is quite linear between 0.1 and 1 M water.

All of the quantities in eq 13 are known except for $f_{HO_2^-}f_{OH^-}$, so this product was calculated for each concentration of water. It was found that, above 0.1 M, the logarithm of $f_{HO_2^-}f_{OH^-}$ varied linearly with the logarithm of the water concentration. The line in Figure 10 is based on the linear regression equation, $\log(f_{HO_2^-}f_{OH^-}) = -(9.15)\log([H_2O]) - 10.02$ ($R = 0.9996$). According to this approach, the value of $f_{HO_2^-}f_{OH^-}$ becomes quite small (10^{-10} at 1 M water), which is indicative of strong hydrogen-bonding interactions between water and the products HO_2^- and OH^-, particularly the latter, we suspect.

The shift in formal potential due to the first term in brackets in eq 13 is quite modest: only 59 mV on going from 0.1 to 1.0 M water. Most of the shift is due to the third term that contains the fractions of the species present in the free form. Thus the combined hydrogen-bonding interactions between water and the two ionic products, HO_2^- and OH^-, greatly exceeds the interaction between water and the reactant, $O_2^{-\bullet}$.

Similar analyses could be performed on the shifts of the second peak potential seen upon the addition of methanol and 2-propanol (Figure 8). The analysis would be hampered somewhat by our lack of knowledge of the standard potentials for the analogues to eq 11. However, qualitatively one can state that the larger shifts seen for methanol compared to water must represent stronger hydrogen bonding interactions between the product ions, HO_2^- and CH_3O^-, and methanol as compared to the analogous interactions in the case of water. Similarly, these interactions must be weaker than those with water for the case of 2-propanol in order to explain the smaller shifts (Figure 8).

4. Conclusion

The reduction of dioxygen in ACN in the presence of hydroxylic additives (water, methanol, and 2-propanol) occurs by a quasireversible one-electron reaction with formation of hydrogen-bonded complexes between the product superoxide and the additive. Formation constants for 1:1 and 1:2 (superoxide/additive) complexes have been evaluated. The complexed superoxide is the reactant at the second stage of reduction, and the irreversible one-electron reduction occurs by a CPET reaction producing HO_2^- and the anion of the additive. The apparent value of the electron-transfer coefficient, α, is unusually small (0.19), which is consistent with a quadratic barrier-driving force relationship and the fact that the second peak occurs at potentials corresponding to a high driving force. A significant KIE is seen for higher concentrations of H_2O/D_2O, CH_3OH/CH_3OD, and $(CH_3)_2CHOH/(CH_3)_2CHOD$, an observation that is consistent with a CPET reaction. Finally, the second irreversible reduction peak moves to less negative values as the additive concentration increases. The peak potentials have been analyzed by assuming that the standard rate constant and the reorganization energy are independent of water concentration and that the shift is due to the effect of water on the formal potential. This occurs because water is a reactant and because of stronger hydrogen-bonding interactions between water and the product ions, HO_2^- and OH^-, compared to the interactions with the reactant superoxide.

Acknowledgment. This research was supported by the National Science Foundation, Grant CHE 0347471.

Supporting Information Available: Estimation of the standard potential for the electrochemical reduction of dioxygen in ACN. This material is available free of charge via the Internet at http://pubs.acs.org.

References and Notes

(1) Tarasevich, M. R.; Sadkowski, A.; Yeager, E. In *Comprehensive Treatise of Electrochemistry*; Conway, B. E., Bockris, J. O'M., Yeager, E., Khan, S. U. M., White, R. E., Eds.; Plenum: New York, 1983; Vol. 7, pp 301−398.

(2) *Frontiers of Cellular Bioenergetics*; Papa, S., Guerrieri, F., Tager, J. M., Eds.; Kluwer/Plenum: New York, 1999.

(3) Kê, B. *Advances in Photosynthesis*; Kluwer: Dordrecht, The Netherlands, 2001; Vol. 10.

(4) Rabani, J.; Nielsen, S. O. *J. Phys. Chem.* **1969**, *73*, 3736−3744.

(5) Chevalet, J.; Rouelle, F.; Gierst, L.; Lambert, J. P. *J. Electroanal. Chem.* **1972**, *39*, 201−216.

(6) Kastening, B.; Kazemifard, G. *Ber. Bunsen-Ges. Phys. Chem.* **1970**, *74*, 551−556.

(7) Divišek, J.; Kastening, B. *J. Electroanal. Chem.* **1975**, *65*, 603−621.

(8) Buess-Herman, C.; Gierst, L. *Electrochim. Acta* **1984**, *29*, 303−309.

(9) Yang, H.-H.; McCreery, R. L. *J. Electrochem. Soc.* **2000**, *147*, 3420−3428.

(10) Matsumoto, F.; Okajima, T.; Uesugi, S.; Koura, N.; Ohsaka, T. *Electrochemistry* **2003**, *71*, 266−273.

(11) Maricle, D. L.; Hodgson, W. G. *Anal. Chem.* **1965**, *37*, 1562−1565.

(12) Sawyer, D. T.; Roberts, J. L. *J. Electroanal. Chem.* **1966**, *12*, 90−101.

(13) Peover, M. E.; White, B. S. *Electrochim. Acta* **1966**, *11*, 1061−1067.

(14) Peover, M. E.; Powell, J. S. *J. Polarogr. Soc.* **1966**, *12*, 106−108.

(15) Lorenzola, T. A.; López, B. A.; Giordano, M. C. *J. Electrochem. Soc.* **1983**, *130*, 1359−1365.

(16) Matsumoto, F.; Uesugi, S.; Harada, M.; Koura, N.; Ohsaka, T. *Electrochemistry* **2003**, *71*, 927−932.

(17) Ortiz, M. E.; Núñez-Vergara, L. J.; Squella, J. A. *J. Electroanal. Chem.* **2003**, *549*, 157−160.

(18) Al Nashef, I. M.; Leonard, M. L.; Kittle, M. C.; Matthews, M. A.; Weidner, J. W. *Electrochem. Solid-State Lett.* **2001**, *4*, D16−D18.

(19) Buzzeo, M. C.; Klymenko, O. V.; Wadhawan, J. D.; Hardacre, C.; Seddon, K. R.; Compton, R. G. *J. Phys. Chem. A* **2003**, *107*, 8872−8878.

(20) Evans, R. G.; Klymenko, O. V.; Saddoughi, S. A.; Hardacre, C.; Compton, R. G. *J. Phys. Chem. B* **2004**, *108*, 7878−7886.

(21) Zhang, D.; Okajima, T.; Matsumoto, F.; Ohsaka, T. *J. Electrochem. Soc.* **2004**, *151*, D31−D37.

(22) Andrieux, C. P.; Hapiot, P.; Savéant, J.-M. *J. Am. Chem. Soc.* **1987**, *109*, 3768−3775.

(23) Matsumoto, F.; Uesugi, S.; Harada, M.; Koura, N.; Ohsaka, T. *Electrochemistry* **2003**, *71*, 927−932.

(24) Goolsby, A. D.; Sawyer, D. T. *Anal. Chem.* **1968**, *40*, 83−86.
(25) Vasudevan, D.; Wendt, H. *J. Electroanal. Chem.* **1995**, *192*, 69−74.
(26) Guo, Z.; Lin, X. *J. Electroanal. Chem.* **2005**, *576*, 95−103.
(27) (a) We prefer CPET over the term proton-coupled electron transfer (PCET), which can refer to either concerted or stepwise processes (see refs 27b and c). (b) Costentin, C.; Evans, D. H.; Robert, M.; Savéant, J.-M.; Singh, P. S. *J. Am. Chem. Soc*. **2005**, *127*, 12490−12491. (c) Costentin, C.; Robert, M.; Savéant, J.-M. *J. Phys. Chem.*, submitted for publication.
(28) Gritzner, G.; Kuta, J. *Electrochim. Acta* **1984**, *29*, 869−873.
(29) Sawyer, D. T.; Chlercato, G.; Angelis, C. T.; Nanni, E. J.; Tsuchlya, T. *Anal. Chem.* **1982**, *54*, 1720−1724.
(30) Nelsen, S. F.; Chen, L.-J.; Petillo, P. A.; Evans, D. H.; Neugebauer, F. A. *J. Am. Chem. Soc*. **1993**, *115*, 10611−10620.
(31) (a) The principles used to derive eq 6 are the same as those used to interpret the half-wave potentials of metal complexes (see ref 31b). (b) Heyrovský, J.; Kůta, J. *Principles of Polarography*; Academic Press: New York, 1966; pp 152−155.
(32) Bordwell, F. G. *Acc. Chem. Res*. **1988**, *21*, 456−463.
(33) Bordwell, F. G.; Cheng, J.-P. *J. Am. Chem. Soc.* **1991**, *113*, 1736−1743.
(34) (a) Bard, A. J.; Faulkner, L. R. *Electrochemical Techniques. Fundamentals and Applications*, 2nd ed.; Wiley: New York, 2001; p 236. (b) p 121.